haematologica
Journal of the Ferrata Storti Foundation

IGLV3-21^{R110}-directed bispecific antibodies activate T cells and promote killing in a high-risk subset of chronic lymphocytic leukemia

by Claudia Fischer, Shih-Shih Chen, Johanna Nimmerfroh, Anne Eugster, Simon Stücheli, Christoph Schultheiß, Corinne Widmer, Dominik Heim, Benjamin Kasenda, Jakob Passweg, Sebastian Kobold, Lukas Egli, Nicolò Coianiz, Obinna Chijioke, Nicholas Chiorazzi, Marie Follo, Heinz Läubli, Matthias Peipp and Mascha Binder

Received: February 27, 2025.
Accepted: September 1, 2025.

Citation: Claudia Fischer, Shih-Shih Chen, Johanna Nimmerfroh, Anne Eugster, Simon Stücheli, Christoph Schultheiß, Corinne Widmer, Dominik Heim, Benjamin Kasenda, Jakob Passweg, Sebastian Kobold, Lukas Egli, Nicolò Coianiz, Obinna Chijioke, Nicholas Chiorazzi, Marie Follo, Heinz Läubli, Matthias Peipp and Mascha Binder. IGLV3-21^{R110}-directed bispecific antibodies activate T cells and promote killing in a high-risk subset of chronic lymphocytic leukemia.
Haematologica. 2025 Sept 11. doi: 10.3324/haematol.2025.287697 [Epub ahead of print]

IGLV3-21^{R110}-directed bispecific antibodies activate T cells and promote killing in a high-risk subset of chronic lymphocytic leukemia

Claudia Fischer[1,2], Shih-Shih Chen[3], Johanna Nimmerfroh[1,4], Anne Eugster[1, 2], Simon Stücheli[1,2], Christoph Schultheiß[1,2], Corinne Widmer[5], Dominik Heim[5], Benjamin Kasenda[1], Jakob Passweg[5], Sebastian Kobold[6,7,8], Lukas Egli[9], Nicolò Coianiz[9], Obinna Chijioke[9,10], Nicholas Chiorazzi[3], Marie Follo[11], Heinz Läubli[1,4], Matthias Peipp[12], Mascha Binder[1,2]

[1] Division of Medical Oncology, University Hospital Basel, Basel, Switzerland

[2] Laboratory of Translational Immuno-Oncology, Department of Biomedicine, University and University Hospital Basel, Basel, Switzerland

[3] Institute of Molecular Medicine, The Feinstein Institutes for Medical Research, Northwell Health, Manhasset, NY, USA

[4] Laboratory of Cancer Immunotherapy, Department of Biomedicine, University of Basel and University Hospital Basel, Basel, Switzerland

[5] Division of Hematology, University Hospital Basel, Basel, Switzerland

[6] Division of Clinical Pharmacology, Klinikum der Universität München, Munich, Germany

[7] German Cancer Consortium (DKTK), Partner Site Munich, Munich, Germany

[8] Einheit für Klinische Pharmakologie (EKLiP), Helmholtz Munich, Research Center for Environmental Health (HMGU), Neuherberg, Germany

[9]Cellular Immunotherapy, Institute of Experimental Immunology, University of Zurich, Zurich, Switzerland

[10] Institute of Pathology and Medical Genetics, University Hospital Basel, Basel, Switzerland

[11] Lighthouse Core Facility, Department of Medicine I, Medical Center of the University of Freiburg, Freiburg, Germany

[12] Division of Antibody-Based Immunotherapy, Department of Medicine II, Kiel University, Kiel, Germany

Short title: IGLV3-21^{R110} T cell engager in CLL

Correspondence to:
Mascha Binder, MD, Division of Medical Oncology, University Hospital Basel, Petersgraben 4, 4031 Basel, Switzerland
Phone (+) 41 79 416 5839
E-mail: Mascha.Binder@usb.ch

DATA AVAILABILITY

Sequences of the humanized anti-R110 Fab are publicly available (EP 4 227 322 A1).

ACKNOWLEDGEMENTS

We acknowledge Anja Muskulus for the production of the R110-bsAb as well as the flow cytometry core facility at the Department of Biomedicine, Mihaela Barbu-Stevanovic, Cécile Cumin and Morgane Hilpert, for assistance with the generation of flow cytometry data.

FUNDING

This work was supported by the Swiss National Science Foundation (SNSF) [10.001.762] (to M.B.).

AUTHOR CONTRIBUTIONS

Idea & design of research project: MB, MP; Supply of critical material (e.g. patient material, mouse models, cohorts): MP, SK, CW, DH, BK, JP, OC, NCh, HL; Establishment of Methods: MP, CS, CF, OC, NCh; Experimental work: CF, SC, JN, SS, LE, NC, MF; Analysis and interpretation of primary data: MB, CF, SC, JN, LE, NC, CS; Drafting of manuscript: MB, CF, AE, SS, CS. All authors reviewed and revised the manuscript.

CONFLICT OF INTEREST STATEMENT

The authors disclose no potential conflicts of interest.

ABSTRACT

We previously used a disease-specific B cell receptor (BCR) point mutation (IGLV3-21^{R110}) for selective targeting of a high-risk subset of chronic lymphocytic leukemia (CLL) with chimeric antigen receptor (CAR) T cells. Since CLL is a disease of the elderly and a significant fraction of patients is not able to physically tolerate CAR T cell treatment, we explored bispecific antibodies as an alternative for precision targeting of this tumor mutation. Heterodimeric IgG1-based antibodies consisting of a fragment crystallizable region (Fc) attached to both an anti-IGLV3-21^{R110} Fab and an anti-CD3 (UCHT1) single chain variable fragment (R110-bsAb) selectively killed cell lines engineered to express high levels of the neoepitope as well as primary CLL cells using healthy donor and CLL patient-derived T cells as effectors. R110-bsAb spared polyclonal human B cells (as opposed to CD19-targeting Blinatumomab) as well as CD34^{+} human stem cells. Yet, R110-bsAb induced lower T cell activation than Blinatumomab with primary CLL cells likely due to lower expression of target antigen. *In vivo*, R110-bsAb specifically killed IGLV3-21^{R110}-expressing cell lines and CLL cells while sparing peripheral blood mononuclear cells. These findings highlight bispecific antibodies as a potential off-the-shelf immunotherapy for high-risk CLL patients, offering selective targeting while preserving healthy B cells.

INTRODUCTION

The treatment landscape for chronic lymphocytic leukemia (CLL) has undergone profound changes, evolving from predominantly chemotherapy and antibody combinations to the use of small molecule inhibitors targeting the B cell receptor (BCR) and BCL2 pathways (1-3). With these novel therapies, life expectancy is now approaching that of the general population (3). However, certain patient subsets do not yet experience the same benefits, highlighting the need for novel treatment options (3). These include patients from stereotypic BCR subsets, which may have a poor prognosis and derive only limited long-term benefits from current approaches, including BCR pathway-targeted therapies (4-6).

Stereotypic subsets are characterized by distinct complementarity-determining region 3 (CDR3) sequence motifs, oligomeric membrane organization, and autonomous signaling through BCR-BCR interactions (1, 7-11). Stereotypy may also extend to the BCR's light chain (10, 12, 13). The IGLV3-21^{R110} subset is one such light chain-defined subset that typically exhibits an aggressive clinical course (11, 13-16). IGLV3-21^{R110} is expressed in 10-15% of unselected CLL patients but is overrepresented in cases requiring treatment (13, 16). Functionally, the G-to-R exchange at position 110 of the IGLV3-21 light chain, along with several conserved amino acids in the heavy chain, confers autonomous signaling capacity to the BCR by mediating self-interactions (13, 14, 16).

Since the IGLV3-21^{R110} BCR is specific to CLL and acts as a critical tumor driver, we hypothesized that targeting this receptor would spare normal B cells and that it bears a low risk of epitope escape due to its functional relevance. Additionally, the absence of persistent B cell aplasia could reduce infection-related complications and preserve vaccination responses (17). To this end, we previously developed IGLV3-21^{R110}-targeted CAR T cells and demonstrated their function *in vitro* and *in vivo*, providing proof-of-concept that this targeting approach may be feasible (18).

In this study, we investigated whether our precision therapy approach could be adapted into an off-the-shelf bispecific antibody format to extend its applicability to a broader range of CLL patients, including those too frail for CAR T cell therapy.

METHODS

Details of the methods are provided in the *Online Supplementary Appendix*.

Cell lines, primary CLL and healthy donor blood cells

Cell lines (DMSZ) and IGLV3-21^{R110} or IGLV3-21^{G110} light chain expressing variants thereof were generated as previously described (18). Blood samples from CLL patients were collected after informed consent as approved by the ethics committees of the Universities of Hamburg–Eppendorf, Halle-Wittenberg and Basel. The clinical characteristics of these patients are displayed in Supplementary Table 1. PBMCs were isolated by Ficoll gradient centrifugation. If necessary, Pan T cells, Pan B cells or CD34^{+} hematopoietic stem cells were additionally isolated via magnetic-activated cell sorting (MACS, Miltenyi Biotec).

Bispecific antibody constructs

The bispecific antibody construct is derived from the humanized antigen-binding fragment (Fab) of the IGLV3-21^{R110}-specific antibody from AVA Lifescience GmbH (Denzlingen, Germany; patent EP 4 227 322 A1). The R110 bispecific antibody (R110-bsAb) was designed as heterodimeric IgG1-based antibody consisting of a fragment crystallizable region (Fc) with knob-into-whole mutations (19) attached to an anti-IGLV3-21^{R110} Fab and an anti-CD3 (UCHT1) single chain variable fragment (anti-CD3 scFv). L234A and L235A point mutations were induced to reduce unspecific Fc-FcR interactions (20).

Bispecific antibody production and purification

Antibody production was performed using CHO-S cells and the MaxCyte STX Scalable Transfection Systems (21) (22). For purification, antibody was isolated from supernatant

with Capture Select^{TM} CH1 Affinity Matrix (Thermo Fisher Scientific). Multimers were excluded *via* size exclusion chromatography using the Äkta Chromatography System (Cytiva). Blinatumomab was used as positive control (23).

In vitro cytotoxicity assay and cytokine quantification

For *in vitro* cytotoxicity assays, 2x10^4 target cells (NALM-6 Luc (-R110), NALM-6, RAJI or OCI-LY1 (G110/R110)) or 4x10^4 primary CLL cells were used. bsAb-dependent T cell activation was determined using flow cytometry. Target cell lysis and fold-change calculation of activation markers is described in the *Online Supplementary Appendix.* IFN-γ release was quantified using the LEGENDplex immunoassay (Biolegend).

In vivo killing assays

All studies with mice were performed in accordance with the respective animal welfare regulations, approved by the respective board/committee (the local ethics committee of Basel-Stadt, Switzerland (approval: 3036, license: 1007-2H), the Institutional Animal Care and Use Committee (IACUC) of the Feinstein Institute for Medical Research (approval: 24-1114, AAALAC: 000751) and the veterinary office of the canton of Zurich, Switzerland (license: ZH067/2023)).

For xenografts, activated healthy donor T cells were expanded for 9 days in culture. A total of 10 NSG (NOD/SCID/IL2rγnull) mice were injected subcutaneously (s.c.) into the right flank with 2x10^6 NALM-6 R110 lymphoma cells. On day 7, 3x10^6 expanded healthy donor T cells were injected intravenously either alone or with R110-bsAb (0.5 mg/kg/dose). Afterwards animals were treated biweekly with R110-bsAb for totally 5 times. Tumor volume was measured every 2 to 3 days starting on day 10.

Patient-derived xenograft assays were conducted as described previously (24). After 10 days, the mice were divided equally into three groups (n = 5/group) and treated

intravenously with either PBS, 0.25 µg/g R110-bsAb or 0.25 µg/g Blinatumomab. Bispecific antibodies were further readministered biweekly. After three weeks, mice were sacrificed and spleens were harvested. T and B cell were quantified by flow cytometry.

Lastly, the effect of R110-bsAb on healthy, polyclonal PBMC, was analyzed using 3–5-month-old NFA2 mice that were injected intraperitoneally (i.p.) with $2.5x10^6$ PKH26-labelled PBMCs originating from two different donors, either alone or in presence of 0.25 µg/g of R110-bsAb or Blinatumomab (in total n=18). After 16 hours, the mice were sacrificed, and peritoneal cells were collected via lavage and analyzed by flow cytometry.

RESULTS

Anti-IGLV3-21^{R110} bispecific antibodies mediate epitope-selective tumor cell lysis in vitro

For the treatment of CLL patients with the IGLV3-21^{R110} light chain mutation (R110), we developed a bispecific antibody construct containing a R110-specific binding moiety coupled to the anti-CD3 domain UCHT1 (Fig. 1A).

Cell lines expressing a recombinant BCR containing the IGLV3-21^{R110} or a corresponding wild-type IGLV3-21^{G110} light chain were generated as described in a previous project (Fig. 1B) (18). The conditions for co-culture experiments were set up using the NALM-6 Luc cell line as target cells with different ratios of healthy donor T cells as effector cells (effector to target ratios; E:T) and the anti-CD19 bispecific T cell engager Blinatumomab as positive control at the previously established concentration of 2 nM (Suppl. Fig. 1A)(25, 26). In addition, we used primary R110-negative CLL cells as target cells (Suppl. Fig. 1B). In both settings, an E:T ratio of 5:1 appeared to allow for efficient lysis of both the target cell line and primary CLL cells.

Co-culture of NALM-6 Luc-R110 cells with healthy donor T cells and increasing concentrations of R110-bsAb showed increasing levels of epitope-selective lysis of the NALM-6 Luc-R110 cell line, while control NALM-6 Luc cells were unaffected (Fig. 1C).

Blinatumomab equally lysed both CD19-positive cell lines independently of the R110 epitope (Fig. 1C). Without the addition of bispecific antibodies, only baseline levels of killing were observed. If no effector cells were present or the antibody did not have an anti-CD3 domain, as in the case of the monospecific antibody R110-Ab, no specific killing above baseline occurred (Suppl. Fig. 1C). This suggests that R110-bsAb killing was mediated by engagement of effector T cells (Fig. 1C). Cell lysis was accompanied by expression of CD25 and CD69 on the activated $CD8^+$ T cells (Fig. 1D).

These results were reproducible with alternative B cell lines transduced to express the R110-epitope such as NALM-6 (without Luciferase), OCI-LY1 and RAJI (Supplementary Fig. 2A, B). To confirm specificity for the R110 point mutation, we included for each cell line a variant expressing the IGLV3-21 light chain in wild-type configuration (G110). As expected, these wild-type variants were unaffected by R110-bsAb treatment (Supplementary Fig. 2A, B). The mutation-specific pattern was also observed if IFN-γ secretion was used as a read-out (Fig. 1E). Since the RAJI cell line transduced to express the R110 neoepitope showed lowest killing rates by flow cytometry (Supplementary Fig. 2A), we wished to further corroborate our findings by confocal microscopy. RAJI R110 showed extensive cluster formation upon R110-bsAb treatment suggesting sufficient T cell engagement (Fig. 1F).

T cells lyse primary CLL cells in the presence of R110-directed bispecific antibodies

We chose a CLL case with known R110-expression and a R110-negative case to test our R110-bsAb compared to CD19-directed Blinatumomab in a setting of primary human CLL cells (Fig. 2A). The mean fluorescence intensity (MFI) of the BCR carrying the R110 mutation is notably reduced in primary CLL as compared to transduced cell lines (Fig. 2B). Nevertheless, R110 epitope-specific patterns of cell lysis were observed with primary human CLL cells as targets using the lysis assay described above (Fig. 2C).

Blinatumomab lysed primary CLL cells independently of R110 status (Fig. 2C). R110-bsAb and Blinatumomab dosing required for optimal lysis was higher in this model using primary CLL cells as compared to the cell line model. This was also reproducible when testing the R110-positive cells from a second patient (Supplementary Fig. 3). T cell activation accompanied the observed effects, but Blinatumomab more potently induced T cell activation than R110-bsAb (Fig. 2D, E). We noted very similar activation patterns for CD4 and CD8 (Fig. 2D, E). Since T cell activation by the two T cell engaging antibodies was equal in the cell line model with high expression of the target antigens CD19 and R110, the differences in the assays with primary cells were interpreted to be related to lower R110 antigen density in CLL as previously shown (Fig. 2B) (18).

R110-directed bispecific antibodies spare polyclonal human B cells, peripheral blood mononuclear cells and hematopoietic stem cells

T cells in the presence of R110-bsAb did not lyse and were not activated by polyclonal human B cells (BC) at an E:T ratio of 5:1 (BC, Fig. 3A, B, C). In conditions with Blinatumomab, cell lysis and T cell activation were observed with polyclonal human B cells as target cells as expected (Fig. 3A, B, C).

To explore B cell lysis in a more natural setting, we used healthy donor derived peripheral blood mononuclear cells (PBMC) and treated them with R110-bsAb. The natural E:T ratio in these samples was 9:1 and therefore even higher than in the previous experiments. T cells in the presence of R110-bsAb did not lyse and were not activated by PBMC, while with Blinatumomab lysis and activation were observed (Fig. 3A, B, C).

Since the R110-epitope is tumor-specific, we did not expect any reactivity with normal tissues. To explicitly rule out stem cell toxicity, we included hematopoietic CD34-positive stem cells (HSC) in our co-culture experiment. CD19-negative HSC were isolated from a

leukapheresis product of a human donor by CD34 sorting. As expected, no killing or activation of T cells was observed with R110-bsAb (Fig. 3A, B, C).

CLL patient-derived T cells lyse target cells in the presence of R110-directed bispecific antibodies

To better simulate the patient setting, we next asked if this targeting principle is also applicable to primary CLL T cells. We, therefore, isolated T cells from a total of three CLL patients and three healthy donors and used them as effector cells in co-culture assays using the OCI-LY1 R110 model system. Indeed, the epitope-specific patterns of cell lysis were equally observed with primary CLL-derived T cells as effector cells using the lysis and activation assays described above (Fig. 4A, B, C). Blinatumomab showed epitope-independent killing with primary CLL-derived T cells in this cell line model (Fig. 4A, B, C).

R110-directed bispecific antibodies are efficacious in xenograft IGLV3-21^{R110}-models

Next, we evaluated the *in vivo* efficacy of our R110-bsAb in three different mouse models. We engrafted NSG mice with NALM-6 R110 cells and administered repeated treatments of the R110-bsAb, while untreated mice served as controls (Fig. 5A). Monitoring tumor growth over time, we observed exponential tumor growth in mice without treatment starting 20 days post tumor injection (Fig. 5B). In contrast, tumor growth was effectively suppressed in mice treated with the R110-bsAb (Fig. 5B).

To further validate the therapeutic efficacy of R110-bsAb, a human CLL PBMC xenograft mouse model was generated from R110-positive patient CLL472. NSG mice were injected intravenously with patient CLL472-derived PBMC and T cells in a 40:1 ratio and treated with R110-bsAb or Blinatumomab biweekly for 3 weeks starting 10 days post CLL PBMC injection (Fig. 5C). After sacrificing the mice, the distribution of human $CD3^+$ and $CD19^+$ cells in the mouse spleen was analyzed by flow cytometry. We observed a nearly

complete clearance of B cells form the spleen of R110-bsAb and Blinatumomab treated mice (Fig. 5D, right panel). Mice treated with PBS retained high levels of B cells. Importantly, there was no significant difference between the $CD3^+$ T cell counts after R110-bsAb and Blinatumomab administration (Fig. 5D, left panel).

Lastly, injecting NFA2 mice with human healthy donor polyclonal PBMC and our R110-bsAb revealed no significant reduction of the B cell population compared to the non-injected mice (Fig. 5E, F). In contrast, Blinatumomab treatment led to a significant decrease in B cell numbers compared to pre-injection levels or R110-bsAb treatment (Fig. 5F).

DISCUSSION

Cell-based and bispecific antibody-based immunotherapies have become essential treatment options for patients with B cell lymphomas, achieving long-term remission in many patients (27-34). However, in chronic lymphocytic leukemia (CLL), these therapies are not as widely used as in other lymphomas (35). Currently, only CD19 CAR T cells are approved in the U.S. for CLL, with no bispecific antibody therapies yet approved (31, 35). One challenge in using these treatments is the eradication of the entire B cell lineage, potentially leading to infectious complications and lack of response to vaccination (17, 36). Since CLL patients are often elderly and frail, the applicability of CAR T cell therapy may in general also be somewhat hampered due to more severe side effects compared to bispecific antibodies (37-39). Consequently, there is a need for targeted and tolerable therapeutic approaches especially for patients with high-risk disease.

To address these challenges, we have developed a bispecific T cell engager that targets a recurrent oncogenic point mutation in the BCR light chain of malignant CLL cells. Previously, we demonstrated proof-of-principle with a CAR T cell therapy targeting the same epitope (18). The data presented here show that this bispecific approach is effective,

even when using CLL-derived T cells as effector cells. Importantly, however, our construct selectively spared healthy B cells, similar to the precision targeting seen in our CAR T cell approach (18).

A critical consideration for the clinical translation of our approach is the relatively low surface expression of the mutated B cell receptor on CLL cells (40). In our primary *in vitro* assays, T cell activation and cytotoxicity were consistently lower with our specific bispecific T cell engager than with CD19-directed bispecific antibodies, which likely reflects the reduced antigen density of the R110 target. This highlights the importance of optimizing dosing strategies to ensure sufficient T cell engagement. Indeed, in our *in vivo* model, tumor regrowth was observed eleven days after the final bsAb administration, suggesting that sustained or repeated dosing may be necessary to maintain therapeutic efficacy. Moreover, it is important to acknowledge that *ex vivo* assays in CLL were hampered by technical limitations in this study. CLL cells are notoriously difficult to maintain in culture due to their low intrinsic vitality outside the patient's microenvironment, which can impact the robustness and reproducibility of functional assays. This inherent fragility poses challenges for immunotherapy testing and underscores the need for cautious interpretation of *ex vivo* findings. Despite these challenges, this mutation-directed approach could serve as a valuable addition to existing therapies. In particular, combining lineage-specific targeting (e.g., CD19) with mutation-specific bispecific antibodies may enhance specificity, reduce off-target effects, and provide a strategy to overcome antigen escape or resistance in high-risk CLL subsets such as those carrying the R110 mutation.

Thereby, our research contributes to the broader effort of developing immunotherapies that target restricted, ideally tumor-specific, rather than lineage-specific, surface molecules. Several studies have explored this direction, notably the application of similar concepts to target clonotypic T cell receptors (TCR) in T cell lymphomas with antibody-drug conjugates (41) or bispecific antibodies (42). However, T cell lymphomas are less clonal, with

approximately 50% of cases being oligoclonal for the TCR, which limits the applicability of this strategy (43, 44). Also for CLL, several other more tumor-specific surface molecules are currently being explored for immunotherapy such as Siglec-6 (45) or ROR-1 (46).

One of the major challenges in CLL is T cell dysfunction, which may limit the efficacy of such therapies (38, 39, 47). In our study, we observed little to no reduction in the potency of T cells recruited to lyse target cells when using patient-derived effector cells of three individual CLL patients. Nevertheless, the efficacy of these T cells may vary between individual patients and at different stages of treatment. Before progressing to clinical trials, it will be important to conduct repeated testing with more CLL T cell donors at different disease stages to better understand the factors influencing treatment efficacy. Given that T cell dysfunction worsens over time in these patients (47), it may be advisable to test these strategies early in the course of high-risk IGLV3-21^{R110} disease.

In summary, we provide proof-of-concept for a mutation-targeted bispecific antibody approach in CLL, which warrants further study.

REFERENCES

1. Hallek M, Cheson BD, Catovsky D, et al. iwCLL guidelines for diagnosis, indications for treatment, response assessment, and supportive management of CLL. Blood. 2018;131(25):2745-2760.

2. Bosch F, Dalla-Favera R. Chronic lymphocytic leukaemia: from genetics to treatment. Nat Rev Clin Oncol. 2019;16(11):684-701.

3. Hallek M, Al-Sawaf O. Chronic lymphocytic leukemia: 2022 update on diagnostic and therapeutic procedures. Am J Hematol. 2021;96(12):1679-1705.

4. Agathangelidis A, Darzentas N, Hadzidimitriou A, et al. Stereotyped B-cell receptors in one-third of chronic lymphocytic leukemia: a molecular classification with implications for targeted therapies. Blood. 2012;119(19):4467-4475.

5. Agathangelidis A, Chatzidimitriou A, Gemenetzi K, et al. Higher-order connections between stereotyped subsets: implications for improved patient classification in CLL. Blood. 2021;137(10):1365-1376.

6. Binder M, Müller F, Jackst A, et al. B-cell receptor epitope recognition correlates with the clinical course of chronic lymphocytic leukemia. Cancer. 2011;117(9):1891-1900.

7. Gomes de Castro MA, Wildhagen H, Sograte-Idrissi S, et al. Differential organization of tonic and chronic B cell antigen receptors in the plasma membrane. Nat Commun. 2019;10(1):820.

8. Minici C, Gounari M, Übelhart R, et al. Distinct homotypic B-cell receptor interactions shape the outcome of chronic lymphocytic leukaemia. Nat Commun. 2017;8:15746.

9. Minden MD-v, Übelhart R, Schneider D, et al. Chronic lymphocytic leukaemia is driven by antigen-independent cell-autonomous signalling. Nature. 2012;489(7415):309-312.

10. Stamatopoulos K, Belessi C, Hadzidimitriou A, et al. Immunoglobulin light chain repertoire in chronic lymphocytic leukemia. Blood. 2005;106(10):3575-3583.

11. Stamatopoulos K, Belessi C, Moreno C, et al. Over 20% of patients with chronic lymphocytic leukemia carry stereotyped receptors: pathogenetic implications and clinical correlations. Blood. 2006;109(1):259-270.

12. Kostareli E, Sutton LA, Hadzidimitriou A, et al. Intraclonal diversification of immunoglobulin light chains in a subset of chronic lymphocytic leukemia alludes to antigen-driven clonal evolution. Leukemia. 2010;24(7):1317-1324.

13. Maity PC, Bilal M, Koning MT, et al. *IGLV3-21*01* is an inherited risk factor for CLL through the acquisition of a single-point mutation enabling autonomous BCR signaling. Proc Natl Acad Sci U S A. 2020;117(8):4320-4327.

14. Gemenetzi K, Psomopoulos F, Carriles AA, et al. Higher-order immunoglobulin repertoire restrictions in CLL: the illustrative case of stereotyped subsets 2 and 169. Blood. 2021;137(14):1895-1904.

15. Stamatopoulos B, Smith T, Crompot E, et al. The Light Chain IgLV3-21 Defines a New Poor Prognostic Subgroup in Chronic Lymphocytic Leukemia: Results of a Multicenter Study. Clin Cancer Res. 2018;24(20):5048-5057.

16. Nadeu F, Royo R, Clot G, et al. IGLV3-21R110 identifies an aggressive biological subtype of chronic lymphocytic leukemia with intermediate epigenetics. Blood. 2021;137(21):2935-2946.

17. Wudhikarn K, Perales M-A. Infectious complications, immune reconstitution, and infection prophylaxis after CD19 chimeric antigen receptor T-cell therapy. Bone Marrow Transplant. 2022;57(10):1477-1488.

18. Märkl F, Schultheiß C, Ali M, et al. Mutation-specific CAR T cells as precision therapy for IGLV3-21R110 expressing high-risk chronic lymphocytic leukemia. Nat Commun. 2024;15(1):993.

19. Merchant AM, Zhu Z, Yuan JQ, et al. An efficient route to human bispecific IgG. Nat Biotechnol. 1998;16(7):677-681.

20. Pejchal R, Cooper AB, Brown ME, Vásquez M, Krauland EM. Profiling the Biophysical Developability Properties of Common IgG1 Fc Effector Silencing Variants. Antibodies (Basel). 2023;12(3):54.

21. Lutz S, Klausz K, Albici A-M, et al. Novel NKG2D-directed bispecific antibodies enhance antibody-mediated killing of malignant B cells by NK cells and T cells. Front Immunol. 2023;14:1227572.

22. Steger K, Brady J, Wang W, et al. CHO-S Antibody Titers >1 Gram/Liter Using Flow Electroporation-Mediated Transient Gene Expression followed by Rapid Migration to High-Yield Stable Cell Lines. SLAS Discov. 2015;20(4):545-551.

23. Löffler A, Gruen M, Wuchter C, et al. Efficient elimination of chronic lymphocytic leukaemia B cells by autologous T cells with a bispecific anti-CD19/anti-CD3 single-chain antibody construct. Leukemia. 2003;17(5):900-999.

24. Patten PEM, Ferrer G, Chen S-S, et al. A Detailed Analysis of Parameters Supporting the Engraftment and Growth of Chronic Lymphocytic Leukemia Cells in Immune-Deficient Mice. Front Immunol. 2021;12:627020.

25. Ryan W, Chris P, Paul B, et al. Blinatumomab induces autologous T-cell killing of chronic lymphocytic leukemia cells. Haematologica. 2013;98(12):1930-1938.

26. Lei W, Ye Q, Hao Y, et al. CD19-targeted BiTE expression by an oncolytic vaccinia virus significantly augments therapeutic efficacy against B-cell lymphoma. Blood Cancer J. 2022;12(2):35.

27. Kantarjian H, Stein A, Gökbuget N, et al. Blinatumomab versus Chemotherapy for Advanced Acute Lymphoblastic Leukemia. N Engl J Med. 2017;376(9):836-847.

28. Budde LE, Sehn LH, Matasar M, et al. Safety and efficacy of mosunetuzumab, a bispecific antibody, in patients with relapsed or refractory follicular lymphoma: a single-arm, multicentre, phase 2 study. Lancet Oncol. 2022;23(8):1055-1065.

29. Dickinson MJ, Carlo-Stella C, Morschhauser F, et al. Glofitamab for Relapsed or Refractory Diffuse Large B-Cell Lymphoma. N Engl J Med. 2022;387(24):2220-2231.

30. Thieblemont C, Phillips T, Ghesquieres H, et al. Epcoritamab, a Novel, Subcutaneous CD3xCD20 Bispecific T-Cell-Engaging Antibody, in Relapsed or Refractory Large B-Cell Lymphoma: Dose Expansion in a Phase I/II Trial. J Clin Oncol. 2023;41(12):2238-2247.

31. Siddiqi T, Maloney DG, Kenderian SS, et al. Lisocabtagene maraleucel in chronic lymphocytic leukaemia and small lymphocytic lymphoma (TRANSCEND CLL 004): a multicentre, open-label, single-arm, phase 1-2 study. Lancet. 2023;402(10402):641-654.

32. Tong C, Zhang Y, Liu Y, et al. Optimized tandem CD19/CD20 CAR-engineered T cells in refractory/relapsed B-cell lymphoma. Blood. 2020;136(14):1632-1644.

33. Wang M, Munoz J, Goy A, et al. KTE-X19 CAR T-Cell Therapy in Relapsed or Refractory Mantle-Cell Lymphoma. N Engl J Med. 2020;382(14):1331-1342.

34. Neelapu SS, Locke FL, Bartlett NL, et al. Axicabtagene ciloleucel CAR T-cell therapy in refractory large B-Cell lymphoma. N Engl J Med. 2017;377(26):2531-2544.

35. Borogovac A, Siddiqi T. Transforming CLL management with immunotherapy: Investigating the potential of CAR T-cells and bispecific antibodies. Semin Hematol. 2024;61(2):119-130.

36. Hill JA, Li D, Hay KA, et al. Infectious complications of CD19-targeted chimeric antigen receptor-modified T-cell immunotherapy. Blood. 2018;131(1):121-130.

37. Eichhorst B, Hallek M, Goede V. New treatment approaches in CLL: Challenges and opportunities in the elderly. J Geriatric Oncol. 2016;7(5):375-382.

38. van Bruggen JAC, Martens AWJ, Fraietta JA, et al. Chronic lymphocytic leukemia cells impair mitochondrial fitness in CD8+ T cells and impede CAR T-cell efficacy. Blood. 2019;134(1):44-58.

39. Fraietta JA, Lacey SF, Orlando EJ, et al. Determinants of response and resistance to CD19 chimeric antigen receptor (CAR) T cell therapy of chronic lymphocytic leukemia. Nat Med. 2018;24(5):563-571.

40. Payelle-Brogard B, Magnac C, Alcover A, Roux P, Dighiero G. Defective assembly of the B-cell receptor chains accounts for its low expression in B-chronic lymphocytic leukaemia. Br J Haematol. 2002;118(4):976-985.

41. Nichakawade TD, Ge J, Mog BJ, et al. TRBC1-targeting antibody–drug conjugates for the treatment of T cell cancers. Nature. 2024;628(8007):416-423.

42. Paul S, Pearlman AH, Douglass J, et al. TCR β chain-directed bispecific antibodies for the treatment of T cell cancers. Sci Transl Med. 2021;13(584):eabd3595.

43. Willscher E, Schultheiß C, Paschold L, et al. T-cell receptor architecture and clonal tiding provide insight into the transformation trajectory of peripheral T-cell lymphomas. Haematologica. 2024;110(2):457-469.

44. Thiele B, Schmidt-Barbo P, Schultheiss C, Willson E, Weber T, Binder M. Oligoclonality of TRBC1 and TRBC2 in T cell lymphomas as mechanism of primary resistance to TRBC-directed CAR T cell therapies. Nat Commun. 2025;16(1):1104.

45. Cyr MG, Mhibik M, Qi J, et al. Patient-derived Siglec-6-targeting antibodies engineered for T-cell recruitment have potential therapeutic utility in chronic lymphocytic leukemia. J Immunother Cancer. 2022;10(11):e004850.

46. Townsend W, Leong S, Shah M, et al. Time Limited Exposure to a ROR1 Targeting Bispecific T Cell Engager (NVG-111) Leads to Durable Responses in Subjects with Relapsed Refractory Chronic Lymphocytic Leukemia (CLL) and Mantle Cell Lymphoma (MCL). Blood. 2023;142(Supplement 1):329.

47. Rissiek A, Schulze C, Bacher U, et al. Multidimensional scaling analysis identifies pathological and prognostically relevant profiles of circulating T-cells in chronic lymphocytic leukemia. Int J Cancer. 2014;135(10):2370-2379.

FIGURES LEGENDS

Fig. 1 Precision targeting the IGLV3-21^{R110} neoepitope with bispecific antibodies. A Schematic depiction of the design and mechanism of action of R110-bsAb. Created with BioRender.com. **B** Expression of CD19 and the IGLV3-21^{R110} BCR on the cell surface of NALM-6 Luc and NALM-6 Luc-R110 cell lines. **C** Specific killing of NALM-6 Luc and NALM-6 Luc-R110 target cells via bispecific antibody T cell engagement with an effector cells (E) to target cells (T) (E:T) ratio of 5:1 after 24 h. Healthy Donor (HD) T cells were used as effector cells with Blinatumomab or with the monospecific R110-Ab serving as a control. Killing was normalized to the cell viability of target cells in absence of effector cells or bispecific antibodies. **D** Expression of activation markers CD69 and CD25 on CD8^{+} HD T cells after the 24 h co-culture with NALM-6 Luc or NALM-6 Luc-R110 cells (E:T = 5:1) and a non-serial dilution of bispecific antibodies Blinatumomab, R110-Ab and R110-bsAb. Each point represents the mean of at least two technical replicates with error bars as standard deviation (SD). A non-linear regression analysis was performed to evaluate how specific killing or T cell activation changes upon increasing bsAb concentration. **E** IFN-γ secretion in supernatants harvested after 24 h of co-culture with healthy donor T cells and indicated target cells. **F** Confocal microscopy pictures representative for target-effector cell engagement after 24 h incubation with 2 nM Blinatumomab or R110-bsAb stained with Hoechst for cell nucleus and Nile Red for cytoplasm. T: target cells, E: effector cells.

Fig. 2 Specificity and activity of R110-bsAb against primary CLL cells. A Expression of CD19 and the IGLV3-21^{R110} BCR on the cell surface of primary CLL462 (R110 negative) and CLL472 (R110 positive). **B** Mean Fluorescence Intensity (MFI) of the IGLV3-21^{R110} BCR expression on cell lines and on primary IGLV3-21^{R110} negative and IGLV3-21^{R110} positive CLL cells. **C** Specific target cell lysis of primary target cells CLL462 (R110 negative) and CLL472 (R110 positive) after 24 h of co-culture with HD T cells. An E:T ratio

of 5:1 was used in combination with a non-serial dilution of R110-bsAb or Blinatumomab. Cell lysis was normalized to the cell lysis of target cells without effector cells or bispecific antibody. **D** Percentage of CD69 and CD25 activation marker expressing $CD8^+$ HD T cells after a 24 h co-culture with primary CLL samples (E:T = 5:1) and a non-serial dilution of the bispecific antibodies. **E** Percentage of CD69 and CD25 activation marker expressing $CD4^+$ HD T cells after a 24 h co-culture with primary CLL samples (E:T = 5:1) and a non-serial dilution of bispecific antibodies Blinatumomab and R110-bsAb. Each point represents the mean of two technical replicates with error bars as SD. A non-linear regression analysis was performed to evaluate the effects of increasing bsAb concentration on target cell killing and effector cell activation. T: target cells, E: effector cells.

Fig. 3 Absence of cytotoxic effects of R110-bsAb on the healthy immune cell repertoire and hematopoietic stem cells. A Specific cell lysis of healthy B cells (BC, PBMC) or hematopoietic stem cells (HSC) after 24 h of co-culture with HD T cells in an either allogenic (E:T = 5:1) or autologous (E:T = 9:1) system. For the allogenic systems, target cells were isolated from healthy PBMC and incubated with sorted effector cells and 100 nM Blinatumomab or R110-bsAb. In the autologous system, PBMC were incubated directly after the addition of 100 nM of bispecific antibodies. Cell lysis was normalized to the baseline cell lysis without bispecific antibody. Each dot represents a technical replicate. **B, C** Percentage of activation marker expressing $CD8^+$ (B) or $CD4^+$ (C) T cells after 24 h co-culture of HD T cells cultured with BC, HSC (E:T = 5:1) or PBMC (E:T = 9:1) and a non-serial dilution of Blinatumomab or R110-bsAb. Non-linear regression analyses were performed to highlight the dose-dependent upregulation of T cell activation due to T cell engagement. Each dot represents the mean of at least three technical replicates with error bars as SD. For statistical analysis, an ordinary one-way Analysis of Variance (ANOVA)

combined with a Šidák`s multiple comparisons test was used. T: target cells, E: effector cells, BC: B cells, PBMC: peripheral blood mononuclear cells, HSC: hematopoietic stem cells.

Fig. 4 Comparison of R110-bsAb mediated cytotoxicity and activation of healthy donor or CLL patient-derived T cells. A Specific killing of OCI-LY1-G110 and OCI-LY1-R110 cells after 24 h of co-culture with either HD T cells or CLL T cells (E:T = 5:1) in combination with a non-serial dilution of Blinatumomab or R110-bsAb. **B** Expression of activation markers CD69 and CD25 on $CD8^+$ HD or CLL T cells after 24 h co-culturing with target cells and a non-linear dilution of bispecific antibodies. **C** Expression of activation markers CD69 and CD25 on $CD4^+$ HD or CLL T cells after 24 h co-culturing with target cells and a non-linear dilution of bispecific antibodies. Non-linear regression analyses were performed to demonstrate the dose-response of target cell viability and effector cell activation towards bispecific antibody treatment. Each data point represents the mean of three different CLL patients (CLL424, CLL477, CLL479) or three HDs (HD003, HD169, HD174) with two technical replicates each. Error bars indicate the SD.

Fig. 5 In vivo activity of R110-bsAb. A Workflow of the NALM-6 R110 cell line xenograft model. **B** Growth of NALM-6 R110 tumor cells subcutaneously engrafted in NSG mice untreated or treated with R110-bsAb every 2 to 3 days for 3 weeks. Engrafted mice treated only with T cells served as negative controls. Each data point represents one mouse with the mean tumor volume and error bars as SD. One outlier was identified by Grubbs`Test and removed from the analysis. Statistical analysis was performed using 2way ANOVA combined with a Šidák`s multiple comparisons test. **C** Workflow of the primary human CLL PBMC xenograft model. **D** Percentage of human CD3 and CD19 positive cells derived

from spleens of NSG mice engrafted with primary CLL derived from the IGLV3-21^{R110}-positive CLL donor CLL472. 20 million CLL PBMCs were i.v. injected together with 0.5 million of autologous, activated T cells. Starting on day 10, mice were treated with R110-bsAb, Blinatumomab or PBS twice a week before being sacrificed after 3 weeks. Each data point represents one mouse with error bars as SD. For statistical analysis, a Kruskal-Wallis test was used. **E** Workflow of the primary human PBMC xenograft model. **F** Percentage of human CD19 positive cells in NFA2 mice injected i.p with healthy, polyclonal PBMC +/- R110-bsAb or Blinatumomab. Mice were sacrificed after 16 hours and cells harvested from the peritoneum were analyzed via flow cytometry. Each dot presents one mouse injected with PBMC derived from one donor and each square represents one mouse injected with PBMC derived from another donor with error bars as SD. Statistical analysis was performed using the ordinary one-way ANOVA paired with Tukey`s multiple comparisons test. PBMC: peripheral blood mononuclear cells, s.c.: subcutaneous, i.v.: intravenous, i.p.: intraperitoneal.

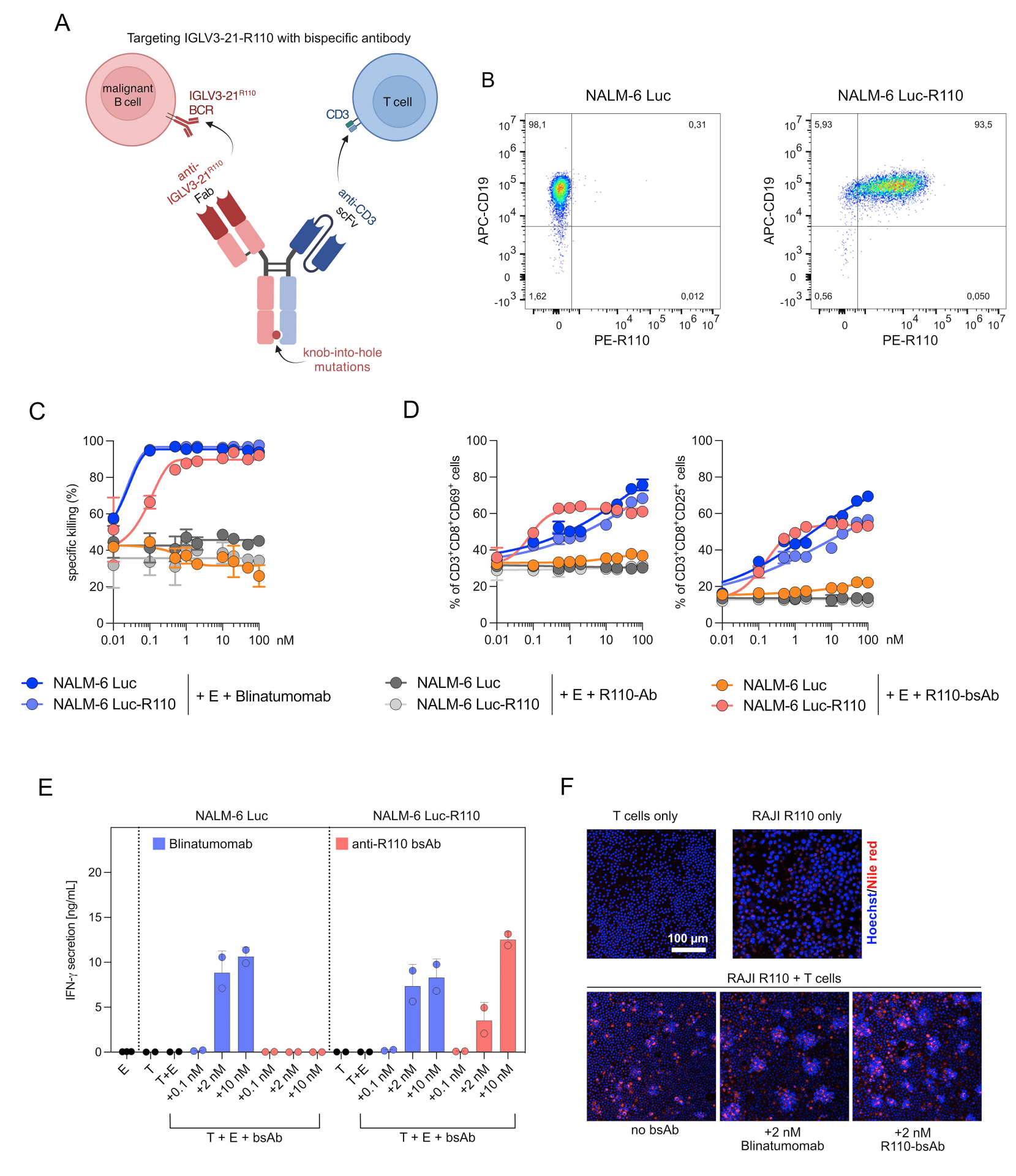
A
Targeting IGLV3-21-R110 with bispecific antibody
malignant B cell
IGLV3-21R110 BCR
T cell
CD3
anti-IGLV3-21R110 Fab
anti-CD3 scFv
knob-into-hole mutations
B
NALM-6 Luc
NALM-6 Luc-R110
APC-CD19
PE-R110
98,1
0,31
1,62
0,012
5,93
93,5
0,56
0,050
C
specific killing (%)
nM
NALM-6 Luc
NALM-6 Luc-R110
+ E + Blinatumomab
D
% of CD3+CD8+CD69+ cells
% of CD3+CD8+CD25+ cells
NALM-6 Luc
NALM-6 Luc-R110
+ E + R110-Ab
NALM-6 Luc
NALM-6 Luc-R110
+ E + R110-bsAb
E
NALM-6 Luc
NALM-6 Luc-R110
Blinatumomab
anti-R110 bsAb
IFN-γ secretion [ng/mL]
E
T
T+E
+0.1 nM
+2 nM
+10 nM
T + E + bsAb
F
T cells only
RAJI R110 only
100 µm
Hoechst/Nile red
RAJI R110 + T cells
no bsAb
+2 nM Blinatumomab
+2 nM R110-bsAb

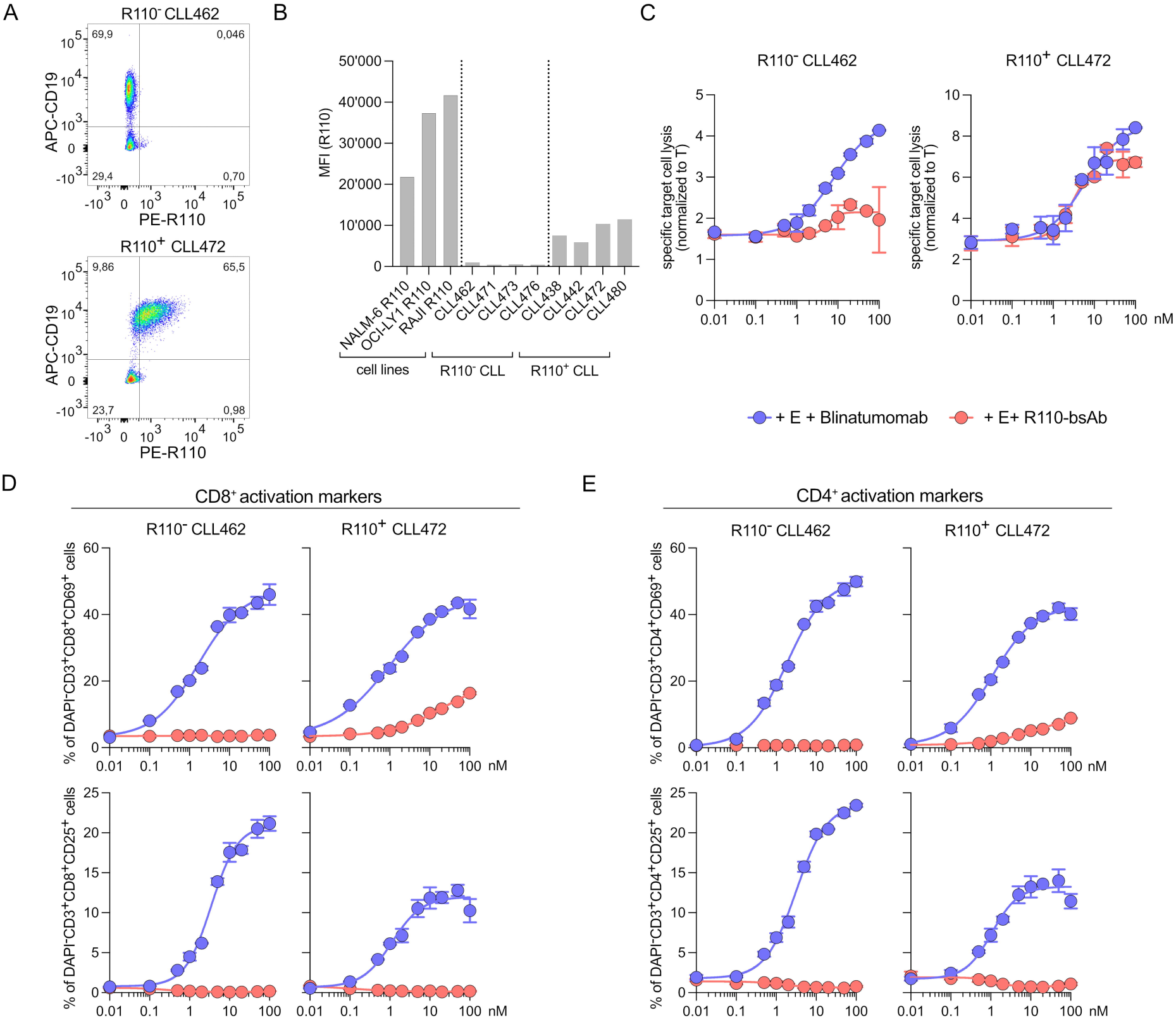
A
R110⁻ CLL462
69,9
0,046
29,4
0,70
APC-CD19
PE-R110
R110⁺ CLL472
9,86
65,5
23,7
0,98
B
MFI (R110)
50'000
40'000
30'000
20'000
10'000
0
NALM-6 R110
OCI-LY1 R110
RAJI R110
CLL462
CLL471
CLL473
CLL476
CLL438
CLL442
CLL472
CLL480
cell lines
R110⁻ CLL
R110⁺ CLL
C
R110⁻ CLL462
R110⁺ CLL472
specific target cell lysis (normalized to T)
nM
+ E + Blinatumomab
+ E+ R110-bsAb
D
CD8⁺ activation markers
R110⁻ CLL462
R110⁺ CLL472
% of DAPI⁻CD3⁺CD8⁺CD69⁺ cells
% of DAPI⁻CD3⁺CD8⁺CD25⁺ cells
nM
E
CD4⁺ activation markers
R110⁻ CLL462
R110⁺ CLL472
% of DAPI⁻CD3⁺CD4⁺CD69⁺ cells
% of DAPI⁻CD3⁺CD4⁺CD25⁺ cells
nM

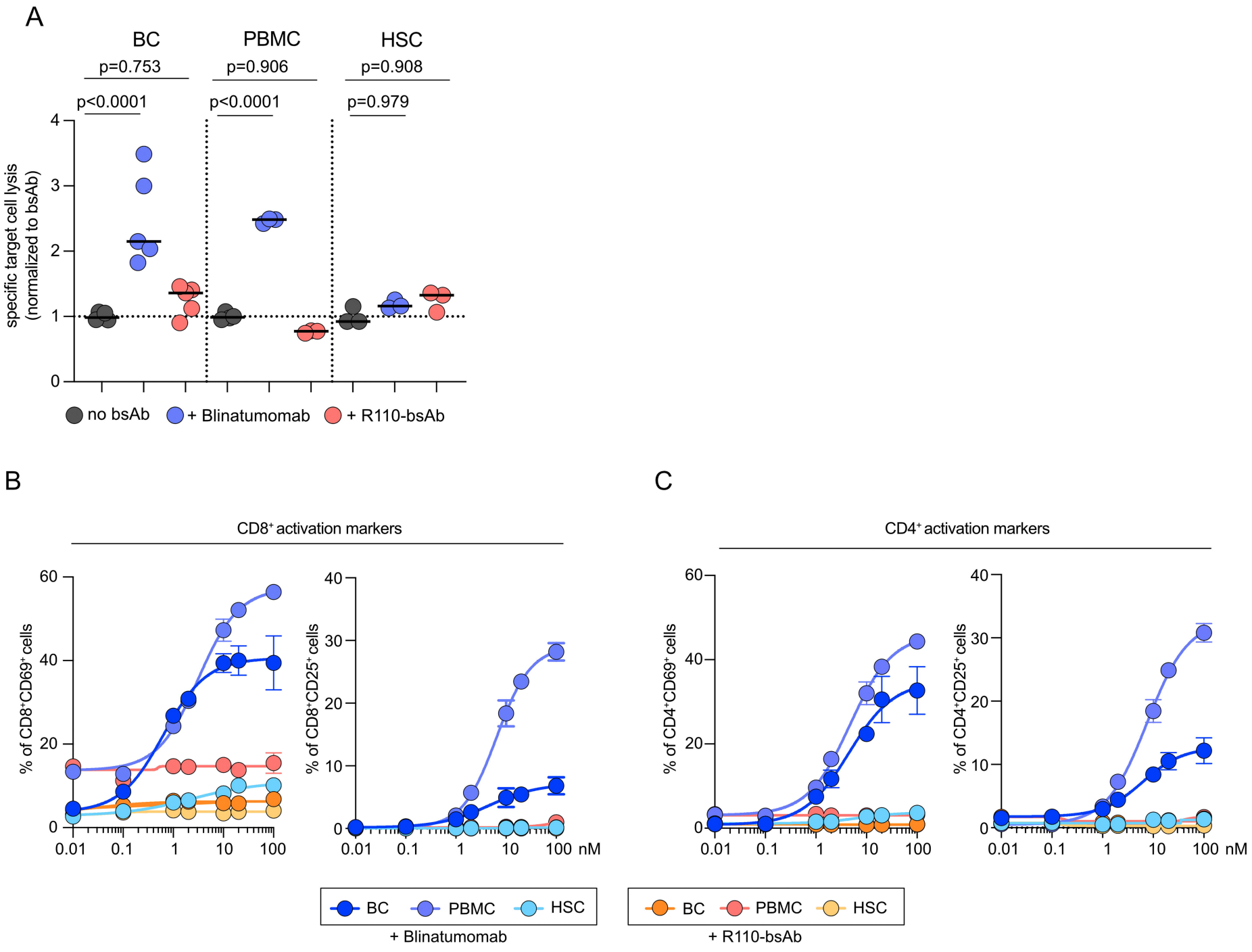
A
BC
PBMC
HSC
p=0.753
p=0.906
p=0.908
p<0.0001
p<0.0001
p=0.979
specific target cell lysis
(normalized to bsAb)
no bsAb
+ Blinatumomab
+ R110-bsAb
B
CD8⁺ activation markers
% of CD8⁺CD69⁺ cells
% of CD8⁺CD25⁺ cells
nM
C
CD4⁺ activation markers
% of CD4⁺CD69⁺ cells
% of CD4⁺CD25⁺ cells
BC
PBMC
HSC
+ Blinatumomab
+ R110-bsAb

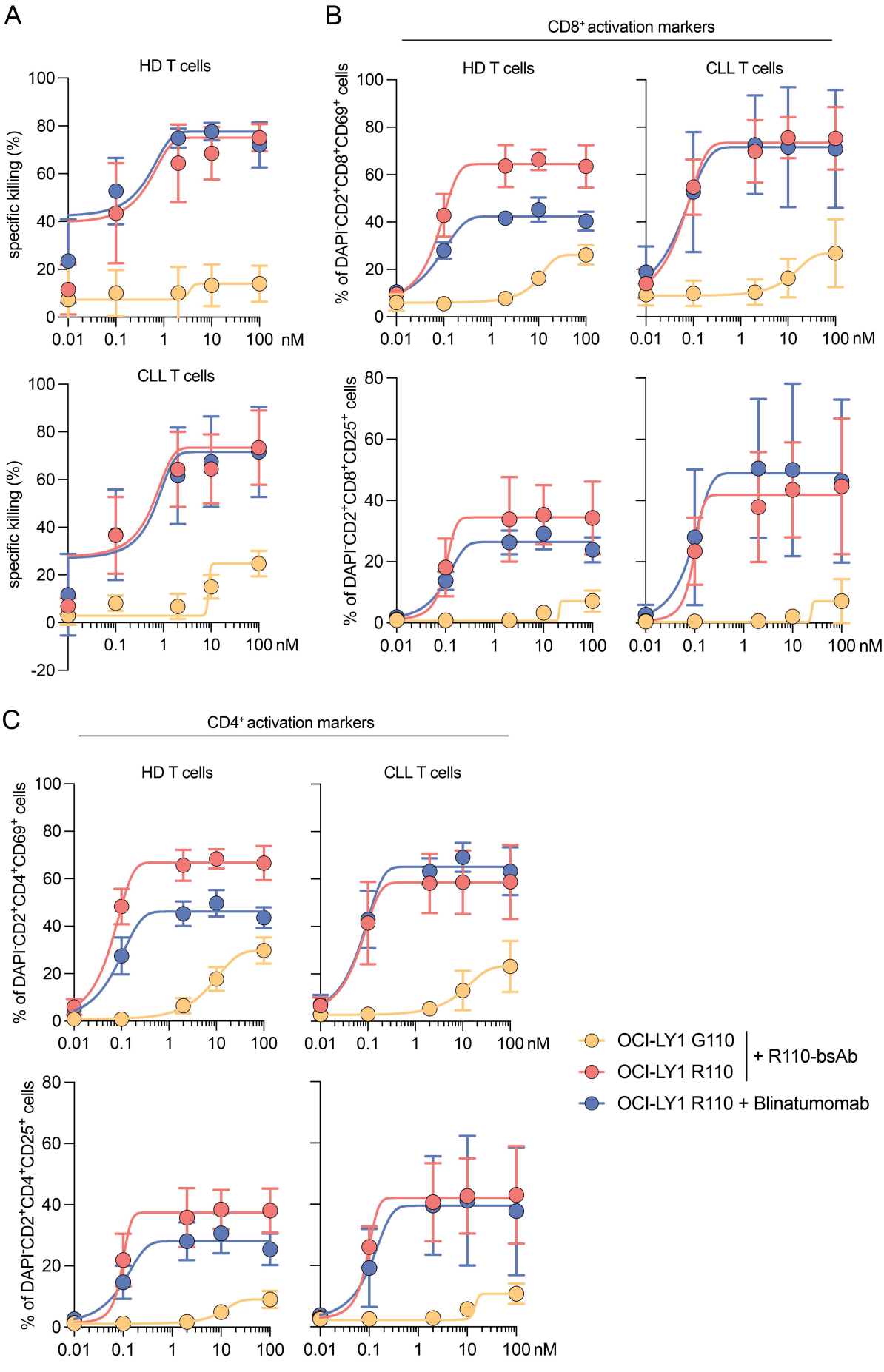
A
HD T cells
CLL T cells
specific killing (%)
100
80
60
40
20
0
-20
0.01
0.1
1
10
100 nM
B
CD8+ activation markers
HD T cells
CLL T cells
% of DAPI-CD2+CD8+CD69+ cells
% of DAPI-CD2+CD8+CD25+ cells
C
CD4+ activation markers
HD T cells
CLL T cells
% of DAPI-CD2+CD4+CD69+ cells
% of DAPI-CD2+CD4+CD25+ cells
OCI-LY1 G110
OCI-LY1 R110
OCI-LY1 R110 + Blinatumomab
+ R110-bsAb

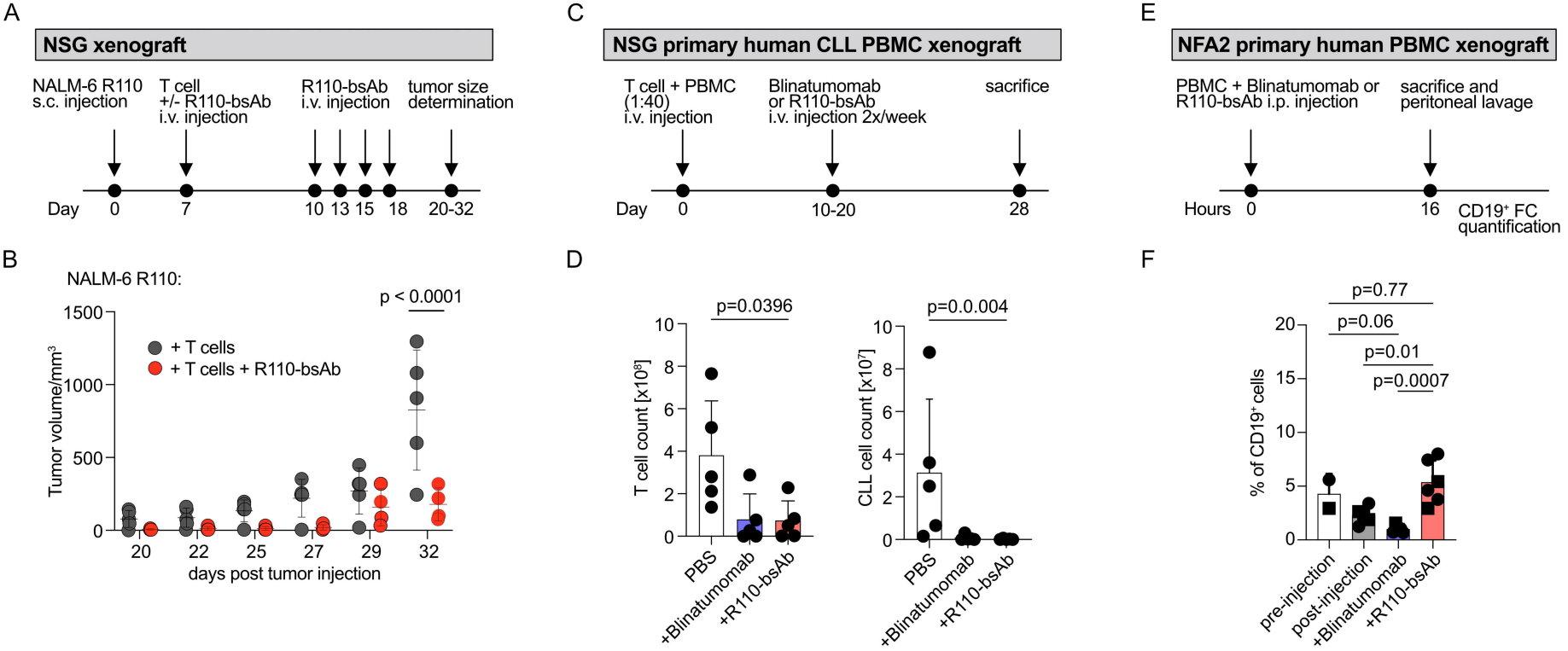
A
NSG xenograft
NALM-6 R110
s.c. injection
T cell
+/- R110-bsAb
i.v. injection
R110-bsAb
i.v. injection
tumor size
determination
Day
0
7
10
13
15
18
20-32
C
NSG primary human CLL PBMC xenograft
T cell + PBMC
(1:40)
i.v. injection
Blinatumomab
or R110-bsAb
i.v. injection 2x/week
sacrifice
Day
0
10-20
28
E
NFA2 primary human PBMC xenograft
PBMC + Blinatumomab or
R110-bsAb i.p. injection
sacrifice and
peritoneal lavage
Hours
0
16
CD19+ FC
quantification
B
NALM-6 R110:
p < 0.0001
+ T cells
+ T cells + R110-bsAb
Tumor volume/mm3
1500
1000
500
0
20
22
25
27
29
32
days post tumor injection
D
p=0.0396
T cell count [x10^8]
p=0.0.004
CLL cell count [x10^7]
PBS
+Blinatumomab
+R110-bsAb
F
p=0.77
p=0.06
p=0.01
p=0.0007
% of CD19+ cells
pre-injection
post-injection
+Blinatumomab
+R110-bsAb

Online Supplementary Appendix

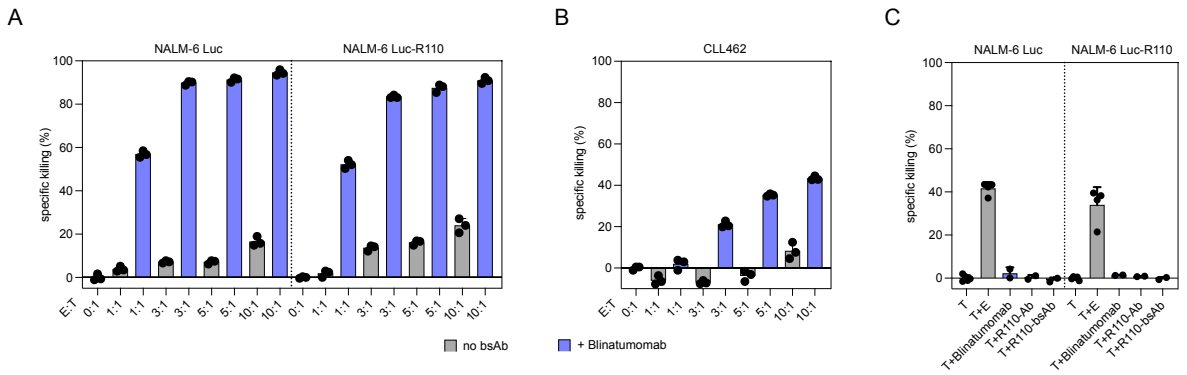

Supplementary Figure 1. Determination of suitable E:T ratios for co-culture experiments. A Specific killing of NALM-6 Luc and NALM-6 Luc-R110 cells incubated at different E:T ratios (0:1, 1:1, 3:1, 5:1, 10:1) with healthy donor (HD) T cells and 2 nM Blinatumomab. **B** Specific killing of primary CLL cells with HD T cells in different E:T ratios (0:1, 1:1, 3:1, 5:1, 10:1) and 5 nM of Blinatumomab. Each bar plot represents the mean of three technical replicates with error bars as SD. **C** Specific killing of NALM-6 Luc and NALM-6 Luc-R110 cells with an E:T ratio of 5:1 after 24 h of incubation with Blinatumomab, the monospecific R110-Ab or R110-bsAb. Each bar plot represents the mean of at least two technical replicates with error bars as SD. E: effector cells, T: target cells, bsAb: bispecific antibody.

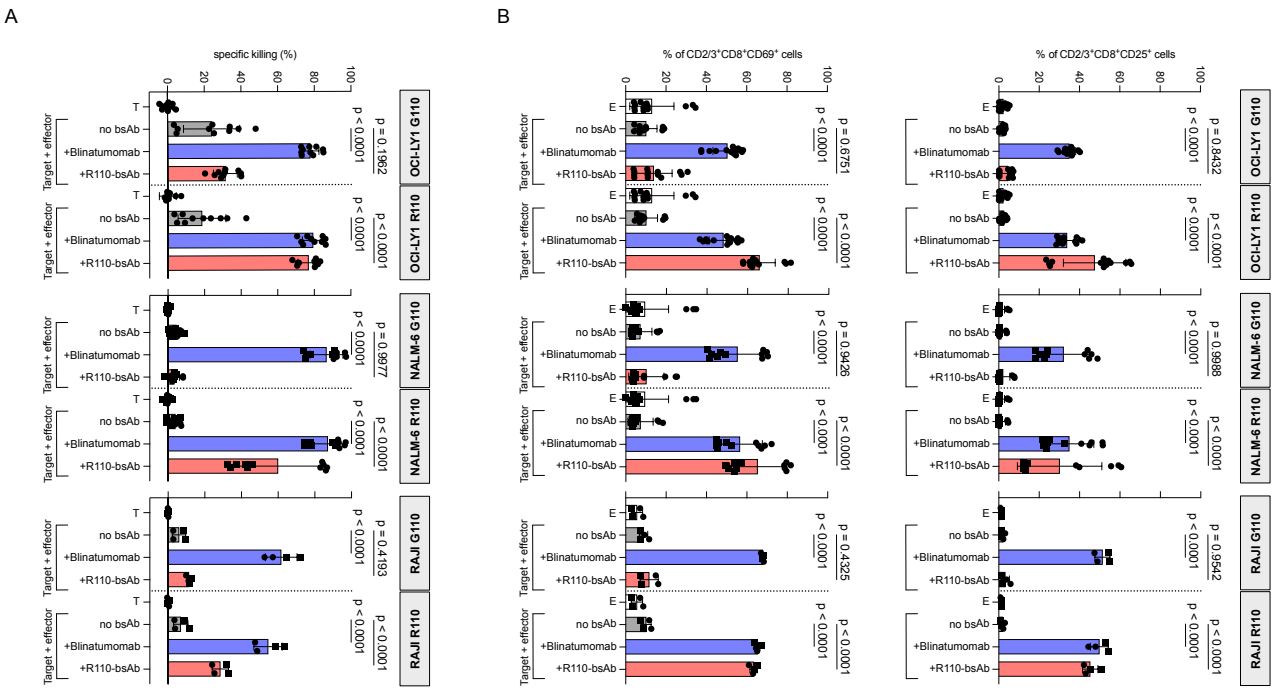

Supplementary Figure 2. Efficacy of R110-bsAb in R110 positive cell line models.

A Specific killing of OCI-LY1 G110/R110, NALM-6 G110/R110 and RAJI G110/R110 cells incubated for 24 h with healthy donor (HD) T cells in a 5:1 ratio and 2 nM bispecific antibodies. **B** Percentage of activation marker expressing $CD8^+$ HD T cells after 24 h of co-culture with different target cells and treated with 2 nM Blinatumomab or R110-bsAb. Dots and squares are technical replicates representative for two different healthy donors used derived from N = 4 (OCI-LY1 G110/R110), N = 3 (NALM-6 G110/R110) or N = 1 (RAJI G110/R110) independent experiments and error bars as SD. Statistical significances were determined by ordinary one-way ANOVA combined with a Šidák`s multiple comparisons test. T: target cells, E: effector cells, bsAb: bispecific antibody.

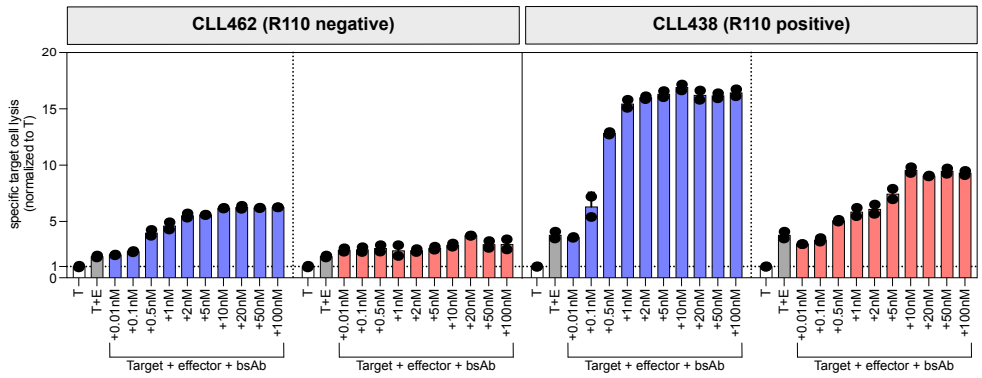

Supplementary Figure 3. Efficacy of R110-bsAb in primary CLL. Specific cell lysis of CLL462 and CL438 target cells with healthy donor (HD) T cells in a 5:1 E:T ratio incubated for 48 h with a non-serial dilution of Blinatumomab or R110-bsAb. Cell Lysis was normalized to the cell lysis of target cells without effector cells or bispecific antibody. Each bar plot represents the mean of two technical replicates with error bars as SD. T: target cells, E: effector cells, bsAb: bispecific antibody.

Supplementary Table 1: Clinical characteristics of CLL patients.

Patient	Sex	Age range	Previously treated at time of sampling	IGLV3-21 R110 status
CLL424	f	50-60	yes	positive
CLL438	m	80-90	yes	positive
CLL472	m	79-80	no	positive
CLL462	f	60-70	no	negative
CLL477	m	80-90	no	negative
CLL479	m	undetermined	no	negative

METHODS

Cell lines, primary CLL and healthy donor blood cells

Cell lines (DMSZ) and IGLV3-21^{R110} or IGLV3-21^{G110} light chain expressing variants thereof were generated as previously described (1). Suspension-adapted Chinese hamster ovary (CHO)-S cells purchased from Thermo Fisher Scientific were cultivated in CD CHO-Medium (Thermo Fisher Scientific) with 1% HT Supplement (Thermo Fisher Scientific) and 1% GlutaMax-I (200 mM L-Ala-L-Gln, Thermo Fisher Scientific) added to the medium. For antibody production, they were kept in CD OptiCHO supplemented with 1% GlutaMax-I, 1% Poloxamer 188, and 1% HAT-Supplement (CHO production medium, Thermo Fisher Scientific).

Blood samples from CLL patients were collected after informed consent as approved by the ethics committees of the Universities of Hamburg–Eppendorf, Halle-Wittenberg and Basel. Peripheral blood mononuclear cells (PBMCs) were isolated by Ficoll gradient centrifugation (Cytiva). If necessary, Pan T cells, Pan B cells or CD34^{+} hematopoietic stem cells were additionally isolated via magnetic-activated cell sorting (MACS, Miltenyi Biotec). PBMCs and T cells were resuspended in FCS + 10% Dimethyl sulfoxide (DMSO) and cryopreserved in liquid nitrogen. IGLV3-21^{R110} expression was characterized by next-generation sequencing (NGS) of the light chain loci as previously described (2-11).

Bispecific antibody constructs

The bispecific antibody construct is derived from the humanized antigen-binding fragment (Fab) of the IGLV3-21^{R110}-specific antibody from AVA Lifescience GmbH (Denzlingen, Germany; patent EP 4 227 322 A1). The R110 bispecific antibody (R110-bsAb) was designed as a heterodimeric IgG1-based antibody consisting of a fragment

crystallizable region (Fc) attached to either an anti-IGLV3-21^{R110} Fab or an anti-CD3 (UCHT1) single chain variable fragment (anti-CD3 scFv). Its light and heavy chain fragments were cloned into the pcDNA3.1(+) vector containing a CMV promotor for antibody expression in CHO-S cells. Knob-into-whole mutations (S354C, T366W vs. Y349C, T366S, L368A, Y407V) in the constant fragments (Fc) of its heavy chains facilitate heterodimerization (12). L234A and L235A point mutations were induced to reduce unspecific Fc-FcR interactions (13).

Bispecific antibody production and purification

Antibody production was performed using the MaxCyte STX Scalable Transfection Systems (14). In brief, CHO-S cells were cultivated at 37°C, 6% CO_2, 145 rpm in serum free CD-CHO medium for at least 2 weeks before being transfected via the MaxCyte STX Scalable Transfection System (MaxCyte, (15)). Transfected cells were further incubated at 32°C, 6% CO_2, 145 rpm for 24 h before sodium butyrate (Sigma) was added. During the following days, feed stock solution, which contained 70% CHO CD Efficient Feed A Stock Solution (Thermo Fisher Scientific), 14% Yeastolate TC UF (Becton Dickinson), 3.5% GlutaMax-I(200 mM)

and 12.5% Glucose (450 g/L, Sigma), was added to the cells until the cell viability dropped below 50%. Supernatant containing the antibody was filtered. For purification, antibody was isolated with the Capture Select^{TM} CH1 Affinity Matrix (Thermo Fisher Scientific) following the manufacturer's instructions. Multimers were excluded via size exclusion chromatography using the Äkta Chromatography System (Cytiva). The commercial bispecific antibody Blinatumomab (anti-CD19/anti-CD3, Blincyto®, Amgen) was used as positive control (16).

In vitro cytotoxicity assay and cytokine quantification

For in vitro cytotoxicity assays using NALM-6 Luc (-R110), NALM-6, RAJI or OCI-LY1 (G110/R110) cells, $2x10^4$ target cells were seeded with effector cells in a 96-well plate and co-incubated in complete media (RPMI 1640 Medium, GlutaMAX™ Supplement, 100 U/mL penicillin and 100 mg/mL streptomycin, 50 µM beta-Mercaptoethanol, Thermo Fisher Scientific; 10% Human Serum) at 37°C and 5% CO_2. For primary CLL target cells, $4x10^4$ cells were seeded. The different E:T ratios as well as the bsAb concentrations used for experiments are indicated in the respective figure descriptions. Cell lysis of target cells was determined after 24 hours of co-culture via flow cytometry using a CytoFLEX™ (Beckman Coulter). Deviating incubation periods are indicated in respective figure descriptions. CD22 PE/Dazzle 594 (HIB22), CD2 FITC (TS1/8) and CD3 APC-Cy7 (SK7, BioLegend) or CD3 FITC (SK7, BD Biosciences) as well as DAPI (Miltenyi) were used for differentiation of effector and target cells or live and dead cells. bsAb-dependent T cell activation was determined using CD8 FITC (SK1), CD25 PE (M-A251, BD Biosciences), CD8 BV650 (SK1), CD4 BV605 (SK3), CD25 BV510 (M-A251) and CD69 APC (FN50, BioLegend) antibodies. The FlowJo™ Software (v.10.10.0) was used for flow cytometric analysis. The percentage of specific killing was determined by the following formula:

$$\%_{\text{specific killing}} = 100 \times ((\%\text{Viability}_{\text{untreated cells}} - \%\text{Viability}_{\text{treated cells}}) / \%\text{Vaibility}_{\text{untreated cells}})$$

Specific target cell lysis was calculated by division of the untreated target cell lysis mean and the sample cell lysis with cell lysis being defined as the loss of $CD22^+$ cells. Fold-change of activation marker-expressing effector cells was equally calculated by the division of the percentage of untreated $CD69^+/CD25^+$ effector cells and the percentage of activation marker positive, treated samples. The amount of released

IFN-γ in the supernatant of the 24 h co-culture was quantified using the LEGENDplex bead-based immunoassay (Biolegend) according to the manufacturer`s instructions. For fluorescence imaging, RAJI R110 cells were seeded at twice the usual quantity and incubated for 20 hours at 37°C and 5% CO_2. Following Hoechst and Nile Red staining (1:100, Sigma-Aldrich), images were captured using the Zeiss LSM 710 confocal microscope and the 20x/0.8 Plan-Apochromat objective.

In vivo killing assays

For cell line-based xenograft assays, healthy donor T cells were activated with 25 µL/mL Immunocult Human CD3/CD28/CD2 T cell activator (STEMCELL) and expanded for 9 days in culture in Prime-XV T cell CDM supplemented with 10 ng/ml IL-7 and IL-15. A total of 10 NSG (NOD/SCID/IL2rγnull) mice were injected subcutaneously (s.c.) into the right flank with $2x10^6$ NALM-6 R110 lymphoma cells suspended in Corning® Matrigel® Matrix High Concentration Phenol-Red-Free diluted 1:1 in phenol red-free DMEM without additives. On day 7, $3x10^6$ expanded healthy donor T cells were injected intravenously either alone or with R110-bsAb (0.5 mg/kg/dose). Afterwards cells were treated biweekly with R110-bsAb for a total of 5 times. Tumor volume was measured every 2 to 3 days starting on day 10 and calculated according to the formula: D/2 x d x d, with D and d being the longest and shortest tumor diameter in mm, respectively.

Patient-derived xenograft assays were conducted as described previously (17). For each mouse, $20x10^6$ PBMC were combined with $0.5x10^6$ of pre-activated T cells from the same CLL patient in a 40:1 ratio. T cell activation was achieved via CD3/CD28 dynabeads and recombinant IL-2 (R&D Systems) treatment over a period of 7 days.

The cell mixture was then injected intravenously in a total of 15 NSG mice. After 10 days, the mice were divided equally into three groups (n = 5 per group) and treated intravenously with either PBS, 0.25 µg/g R110-bsAb or 0.25 µg/g Blinatumomab. The bispecific antibodies were further readministered biweekly. After three weeks, the mice were sacrificed and the spleens were harvested. T and B cell populations were quantified by flow cytometry using anti-human CD19 PE-CF594 (HIB19) and anti-human CD3 PE-Cy7 antibodies (SK7, BD Biosciences). Animal studies were performed in compliance with experimental protocols approved by the Institutional Animal Care and Use Committee (IACUC) of the Feinstein Institute for Medical Research.

Lastly, the effect of R110-bsAb on healthy, polyclonal PBMC, was analyzed using 3–5 month old NFA2 (NOD.Cg-*Rag1*^{tm1Mom} *Flt3*^{tm1Irl} *Mcph1*$^{Tg(HLA-A2.1)1Enge}$ *Il2rg*^{tm1Wjl}/J) mice that were injected intraperitoneally (i.p.) with 2.5×10^6 PKH26-labelled PBMCs originating from two different donors, either alone or in the presence of 0.25 μg/g of R110-bsAb or Blinatumomab (in total n = 18). NFA2 mice were housed under a 12 h light/12 h dark cycle (lights on: 6 am, lights off: 6 pm) at temperatures from 21–24 °C with 35–70% humidity. After 16 hours, the mice were sacrificed, and peritoneal cells were collected via lavage and analyzed by flow cytometry. Mice in which PBMC cells could not be detected by flow cytometry were excluded from the dataset to control for unsuccessful i.p. injections. The antibodies anti-human CD19-BUV661 (HIB19, BD Biosciences) and Zombie NIR™ Fixable Viability Kit (Biolegend) were used for the analysis.

Statistical analysis

Ordinary one-way Analysis of Variance (ANOVA) or 2way ANOVA combined with a Šidák`s multiple comparisons testing was used for the comparison of cell lysis of target cells and activation marker expression on effector cells in the absence or presence of bsAb. For *in vivo* anaylsis, the non-parametric Kruskal-Wallis test was used. Non-linear regression models were further utilized to highlight the dose-dependent decrease of target cell viability and increase of T cell activation marker expressing effector cells. For statistical analyses, the GraphPad Prism software (v10.3.0 (461)) was used.

1. Märkl F, Schultheiß C, Ali M, et al. Mutation-specific CAR T cells as precision therapy for IGLV3-21R110 expressing high-risk chronic lymphocytic leukemia. Nat Commun. 2024;15(1):993.

2. Anna O, Anna B, Minna V, et al. Monitoring multiple myeloma by next-generation sequencing of V(D)J rearrangements from circulating myeloma cells and cell-free myeloma DNA. Haematologica. 2017;102(6):1105-11.

3. Paschold L, Simnica D, Brito RB, et al. Subclonal heterogeneity sheds light on the transformation trajectory in IGLV3-21R110 chronic lymphocytic leukemia. Blood Cancer J. 2022;12(3):49.

4. Paschold L, Simnica D, Willscher E, et al. SARS-CoV-2–specific antibody rearrangements in prepandemic immune repertoires of risk cohorts and patients with COVID-19. J Clin Invest. 2021;131(1).

5. Paschold L, Willscher E, Bein J, et al. Evolutionary clonal trajectories in nodular lymphocyte-predominant Hodgkin lymphoma with high risk of transformation. Haematologica. 2021;106(10):2654-66.

6. Schieferdecker A, Oberle A, Thiele B, et al. A transplant “immunome” screening platform defines a targetable epitope fingerprint of multiple myeloma. Blood. 2016;127(25):3202-14.

7. Schliffke S, Akyüz N, Ford CT, et al. Clinical response to ibrutinib is accompanied by normalization of the T-cell environment in CLL-related autoimmune cytopenia. Leukemia. 2016;30(11):2232-4.

8. Schultheiß C, Paschold L, Simnica D, et al. Next-Generation Sequencing of T and B Cell Receptor Repertoires from COVID-19 Patients Showed Signatures Associated with Severity of Disease. Immunity. 2020;53(2):442-55.e4.

9. Schultheiß C, Simnica D, Willscher E, et al. Next-Generation Immunosequencing Reveals Pathological T-Cell Architecture in Autoimmune Hepatitis. Hepatology. 2021;73(4):1436-48.

10. Simnica D, Ittrich H, Bockemeyer C, Stein A, Binder M. Targeting the Mutational Landscape of Bystander Cells: Drug-Promoted Blood Cancer From High-Prevalence Pre-neoplasias in Patients on BRAF Inhibitors. Front Oncol. 2020;10.

11. Thiele B, Kloster M, Alawi M, et al. Next-generation sequencing of peripheral B-lineage cells pinpoints the circulating clonotypic cell pool in multiple myeloma. Blood. 2014;123(23):3618-21.

12. Merchant AM, Zhu Z, Yuan JQ, et al. An efficient route to human bispecific IgG. Nat Biotechnol. 1998;16(7):677-81.

13. Pejchal R, Cooper AB, Brown ME, Vásquez M, Krauland EM. Profiling the Biophysical Developability Properties of Common IgG1 Fc Effector Silencing Variants. Antibodies. 2023;12(3):54.

14. Lutz S, Klausz K, Albici A-M, et al. Novel NKG2D-directed bispecific antibodies enhance antibody-mediated killing of malignant B cells by NK cells and T cells. Front Immunol. 2023;14.

15. Steger K, Brady J, Wang W, et al. CHO-S Antibody Titers >1 Gram/Liter Using Flow Electroporation-Mediated Transient Gene Expression followed by Rapid Migration to High-Yield Stable Cell Lines. SLAS Discov. 2015;20(4):545-51.

16. Löffler A, Gruen M, Wuchter C, et al. Efficient elimination of chronic lymphocytic leukaemia B cells by autologous T cells with a bispecific anti-CD19/anti-CD3 single-chain antibody construct. Leukemia. 2003;17(5):900-9.

17. Patten PEM, Ferrer G, Chen S-S, et al. A Detailed Analysis of Parameters Supporting the Engraftment and Growth of Chronic Lymphocytic Leukemia Cells in Immune-Deficient Mice. Front Immunol. 2021;12.